SAND2019-12824C

Experimental Application of Boundary Condition Compensation Map (from Field to Laboratory Response)

Brandon Zwink, Brett Daniels, Peter Avitabile
Structural Dynamics and Acoustic Systems Laboratory
University of Massachusetts Lowell
One University Avenue
Lowell, Massachusetts 01854

D. Gregory Tipton
Sandia National Laboratories*
Engineering Sciences Center
Albuquerque, New Mexico, USA

ABSTRACT
Vibration qualification testing is performed to evaluate equipment reliability in a laboratory setting. The actual field environment is difficult to accurately replicate in many situations due to dynamic effects of the vibration test fixture boundary conditions which are seldom well understood or included properly. In essence, the device under test, in the laboratory, sees different response depending on the particular laboratory configuration used. Ultimately the device under test must see the appropriate representation of the in-field environment.

A physics-based map between the field and laboratory modal responses was studied analytically. In this paper, experimental data was collected to help validate the results of the analytical study. A two-beam system, representing the fixture and the device under test, was utilized which allows reconfiguration to create different boundary conditions for the device under test. Classical multi-input-multi-output vibration techniques were utilized to calculate a boundary condition compensated excitation for the laboratory system. Modifications where then made to the calculation techniques to test the validity of the physics-based map between the field and laboratory modal responses. Ultimately, field responses were compared to laboratory test responses to determine how well the field dynamics were replicated in the laboratory configuration.

Keywords: Boundary Condition, Fixture Neutralization, Experimental, MIMO

INTRODUCTION

Vibration testing in a laboratory setting is conducted with the goal of replicating the dynamics of a part observed in a field environment. Laboratory vibration testing provides a low risk opportunity to verify durability, design, and function of parts that will be subjected to shocks or random vibration environments in field use. Classical vibration testing, as described by Sharton [1], has been applied for decades in an attempt to replicate dynamic environments on parts in a laboratory setting.

Typically, a device under test (DUT) will be attached to an electro-dynamic shaker or other means of dynamic excitation, such as an acoustic source. The means of physically constraining the DUT during a vibration test are almost certainly modified from the boundary conditions of the DUT during the field environment. Conventional practice has been to design a stiff laboratory test fixture. In reality, no fixture is truly stiff, and even with a stiff fixture, the boundary conditions for the DUT in the laboratory do not match the boundary conditions of the DUT in the field. This discrepancy in boundary conditions between field and laboratory is typically not accounted for or well understood but can cause the laboratory test dynamics to be inaccurate in the form of an over-excitation or an under-excitation of the DUT. This over-excitation and under-excitation of the DUT was recognized by both Daborn [2] and Avitabile [3]. Over-exciting the DUT during vibration testing can result in unnecessary design changes and added weight, while under-exciting the DUT during vibration testing can result in a false confidence in the design and field environment failures.

Multiple methods have recently been introduced to account for boundary condition differences between field and laboratory during vibration testing. These methods include experimental based approaches based on frequency response function (FRF) method such as the impedance matched multi-axis testing (IMMAT) approach developed by Daborn [2] [4] [5] and the

*Sandia National Laboratories is a multimission laboratory managed and operated by National Technology & Engineering Solutions of Sandia, LLC, a wholly owned subsidiary of Honeywell International Inc., for the U.S. Department of Energy's National Nuclear Security Administration under contract DE-NA0003525. This paper describes objective technical results and analysis. Any subjective views or opinions that might be expressed in the paper do not necessarily represent the views of the U.S. Department of Energy or the United States Government.

FIxure NEutralization (FINE) approach developed by Reyes-Blanco [6]. Modal based techniques were also studied by Mayes [7] [8] and Zwink et al. [9]. The experimental FRF based methods have the advantage in that they do not have frequency bandwidth limitations whereas the modal based methods are limited to the number of modes that can be experimentally extracted and discerned with the experimental instrumentation set. The advantages of the modal based methods are that they give a physics-based understanding of the problem and which modes of vibration need to be measured and excited in the laboratory test configuration.

Zwink et al. [10] derived the relationship between field and laboratory test modal responses, which frames the vibration input calculation methods used by the FINE and IMMAT methods into the format utilized in the MPM approach, providing a physics-based understanding of the modal transformation between field and laboratory. The resulting matrix that describes the relationship between field and laboratory test modes was denoted the Modal Amplitude Contribution Map (MACM).

This paper documents an experimental study to help validate the physics described by the MACM. An experimental setup was designed for a two-beam system similar to the analytical model studied by Zwink et al. [10]. Two configurations for the two-beam system were utilized to designate a DUT that could be configured into two different boundary condition configurations. Both a hammer impact and a random/earthquake vibration excitation were then applied to the system in the "field environment" configuration. The system was re-configured into the "laboratory test" configuration and excited utilizing various methodologies. The methodologies tested were to calculate shaker voltage inputs based on raw experimental FRF measurements, experimental model synthesized FRF measurements, and truncated model synthesized FRF measurements. The MACM function was utilized to determine a minimum set of field environment and laboratory test modes to which the problem could be truncated and still achieve accurate results.

DUT responses in the laboratory configuration are then compared to DUT responses in the field configuration. The similarity of the field and laboratory responses on the DUT were utilized as a metric for success as the goal of the laboratory test is to re-create the DUT response of the field under different boundary conditions.

NOMENCLATURE

M	Mass matrix
K	Stiffness matrix
$\bar{M}$	Modal mass
$\ddot{x}$	Physical acceleration (time domain)
$\ddot{X}$	Physical acceleration (frequency domain)
v	Voltage at function generator (time domain)
V	Voltage at function generator (frequency domain)
$\ddot{p}$	Modal acceleration (time domain)
$\ddot{P}$	Modal acceleration (frequency domain)
f	Physical force (time domain)
F	Physical force (frequency domain)
$\bar{f}$	Modal force (time domain)
$\bar{F}$	Modal force (frequency domain)
U	Mode shapes
$^{(F)}$	Denotes "field environment system"
$^{(L)}$	Denotes "laboratory test system"
$\ddot{H}_{ij}$	Frequency response function (acceleration over force)
H_{nj}	Frequency response function (function generator voltage over force)
$\ddot{\bar{H}}$	Modal frequency response function (modal acceleration over modal force)
ω	Frequency (in rad/s)
ω_k	Natural frequency of the k'th mode (in rad/s)
ζ_k	Damping of the k'th mode (ratio to critical)
j	$\sqrt{-1}$
$_i$	Response DOF on DUT
$_j$	Excitation DOF
$_n$	Voltage DOF
$_k$	k'th mode of the system
†	Generalized inverse
^{T}	Transpose

Nomenclature Examples

$\ddot{X}_i^{(F)}$	Acceleration in frequency domain for field environment system at the "i" degrees of freedom
$U_j^{(L)}$	Mode shape matrix for laboratory test system at the "j" degrees of freedom

THEORY

The general theory was presented by Zwink et al. [10] and only summarizing necessary equations are presented in this paper. The theory utilized in this paper is broken into three sections, the first section reviews the calculations utilized to generate a voltage signal to send to the amplifiers that will replicate a desired DUT response. The second section covers the relationships required to synthesize FRFs and responses from a modal model. The third section covers the equation utilized to understand the relationship between field and laboratory modal responses from which the physics-based insight into which modes are important to the process is derived.

Calculating Function Generator Voltage to Achieve Target DUT Response

The theory for the experimental testing utilizes MIMO principles to replicate the DUT dynamics in the laboratory test configuration that were observed in the field environment configuration. The goal is to derive a shaker voltage that is capable of creating the relationship

$$\left\{\ddot{X}_i^{(L)}\right\} = \left\{\ddot{X}_i^{(F)}\right\} \quad (1)$$

Ideally, Equation 1 would hold true not only at the "i" degrees of freedom (DOFs) measured experimentally, but at all DOFs on the DUT including rotation DOFs.

The relationship between the DUT response on the laboratory test system and the excitation forces applied to the laboratory test system can be described as

$$\left[\ddot{\mathrm{H}}_{ij}^{(L)}\right]\left\{F_j^{(L)}\right\} = \left\{\ddot{X}_i^{(L)}\right\} \tag{2}$$

$\ddot{\mathrm{H}}_{ij}^{(L)}$ can be measured experimentally or synthesized from a model. Combining Equations 1 and 2, and re-arranging terms, results in an equation defining the force required on the laboratory test system to produce the field environment excitation on the laboratory test system at the "i" DOFs. The equation is expressed as

$$\left\{F_j^{(L)}\right\} = \left[\ddot{\mathrm{H}}_{ij}^{(L)}\right]^{\dagger}\left\{\ddot{X}_i^{(F)}\right\} \tag{3}$$

This formulation assumes that the "i" DOFs refer to the same reference DOFs on the device under test for both the field and laboratory systems. Analytical studies [10] showed that under certain conditions, Equation 3 results in Equation 1 being satisfied not only for the chosen "i" DOFs, but for all DOFs (including rotation DOFs) of the DUT. The conditions in which all field and laboratory DUT DOFs match are when the number of forces and the number of reference "i" DOFs are greater than or equal to the number of connection DOFs for the DUT. This statement excludes cases where the DUT is directly excited and is limited to cases in which the DUT is being excited through the boundary conditions.

A closed loop vibration controller was not utilized for this study. Instead, the relationship between function generator voltage and laboratory test excitation force was experimentally measured and utilized to calculate the voltage required to achieve a specified force. This function includes the dynamic effects of the shaker, shaker attachment hardware, and amplifier. If the function generator voltage is measured as a response during a MIMO modal characterization test, the resulting FRF between function generator voltage and force would be expressed as

$$\left[\mathrm{H}_{nj}^{(L)}\right]\left\{F_j^{(L)}\right\} = \left\{V_n^{(L)}\right\} \tag{4}$$

Utilizing Equation 3 and 4, an equation to calculate function generator voltage can be derived to create a target set of DUT responses as

$$\left\{V_n^{(L)}\right\} = \left[\mathrm{H}_{nj}^{(L)}\right]\left[\ddot{\mathrm{H}}_{ij}^{(L)}\right]^{\dagger}\left\{\ddot{X}_i^{(F)}\right\} \tag{5}$$

$\mathrm{H}_{nj}^{(L)}$, $\ddot{\mathrm{H}}_{ij}^{(L)}$, and $\ddot{X}_i^{(F)}$ can all be measured experimentally. Alternatively, if an experimental or analytical model exists, $\mathrm{H}_{ij}^{(L)}$ can be synthesized from a model.

Synthesizing FRFs and Responses from a Modal Model

Synthesizing FRFs from a modal model can be a useful tool in structural dynamics. In this study, FRFs were synthesized using specific modes of vibration. To achieve this goal, FRFs were synthesized from modal FRFs. The modal FRFs relate modal forces to modal responses through the equation

$$\left[\ddot{H}_k\right]\{\bar{F}_k\} = \{\ddot{P}_k\} \tag{6}$$

Modal FRFs can be synthesized using the equation

$$\ddot{H}_k(\omega) = \frac{-\omega^2}{\bar{M}_k(-\omega^2 + 2j\omega_k\zeta_k\omega + \omega_k^2)} \tag{7}$$

The physical FRFs relating force and acceleration, $\ddot{H}_{ij}$, can then be synthesized for the selected modes using the relationship

$$\{\ddot{H}_{ij}\} = [U_i]\left[\ddot{H}\right][U_j]^T \tag{8}$$

In Equation 8, the $\ddot{H}_{ij}$ FRF can be synthesized from a chosen selection of modes and not necessarily all of them.

Field to Laboratory Modal Map

The final theoretical concept utilized in this paper is the equation for the Modal Amplitude Contribution Map (MACM). The full theory and derivation for the MACM is covered by Zwink et al. [10], but the resulting equation is presented here as

$$[M\ddot{A}CM] = \left[\ddot{H}^{(L)}\right]\left[U_j^{(L)}\right]^T\left[\left[U_i^{(L)}\right]\left[\ddot{H}^{(L)}\right]\left[U_j^{(L)}\right]^T\right]^{\dagger}\left[U_i^{(F)}\right]\cdot\{\ddot{P}^{(F)}\}^T \tag{9}$$

The MACM describes the relationship between field and laboratory modal responses. Essentially, the $M\ddot{A}CM$ is equivalent to the laboratory modal response, $\ddot{P}^{(L)}$, split into their corresponding field environment modal responses from which they are derived. If the $M\ddot{A}CM$ were summed over each laboratory test mode, the result would be the laboratory environment modal acceleration, $\ddot{P}^{(L)}$.

EXPERIMENTAL SETUP

An aluminum two-beam system was utilized as the experimental test bed for this paper. The shorter beam was designated as the DUT and is 90 1/16" long. The shorter beam was bolted to a longer beam which was 137 5/16" long and served as the boundary conditions for the DUT. Both beams were hollow rectangular aluminum beams. Holes were drilled in the beams to allow for assembly in a number of configurations.

The "field environment" assembly of the beams was a symmetric configuration and is shown in Figure 1.

Figure 1: Field Environment Configuration of Two-Beam System

To create the “laboratory test” configuration, the top beam was moved to the right 12 inches and bolted to the lower beam as shown in Figure 2.

Figure 2: Laboratory Test Configuration of Two-Beam System

The two-beam system was supported using rubber plungers in an attempt to create a “free-free” boundary condition in the horizontal plane to the extent possible experimentally.

The dynamics of the beam were measured and excited only in the horizontal plane in an effort to simplify the dynamics involved and number of modes required. There were 20, roughly evenly spaced, accelerometers attached to the system. There were 8 accelerometers glued to the top beam and 12 to the bottom beam to capture the dynamics of the system.

Four independently excited electro-dynamic shakers were attached to the lower beam. Each shaker had a corresponding drive point accelerometer as well as a force transducer to measure the excitation forces exerted on the system. Each shaker was connected to an amplifier and each amplifier to a function generator capable of generating defined voltage signals. A diagram of accelerometer and shaker placement for the “field environment” configuration can be seen in Figure 3. Similarly, a diagram of accelerometer and shaker placement for the “laboratory test” configuration can be seen in Figure 4.

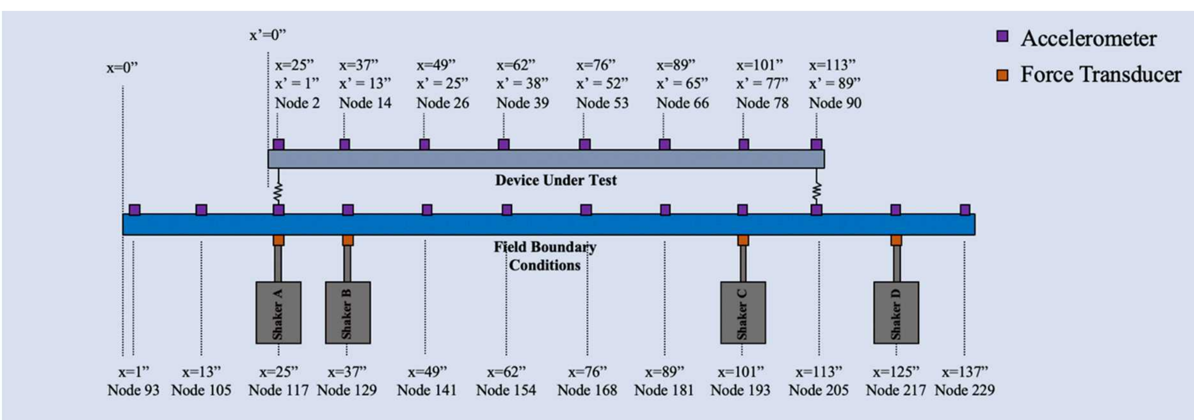

Figure 3: Field Environment Accelerometer and Shaker Placement

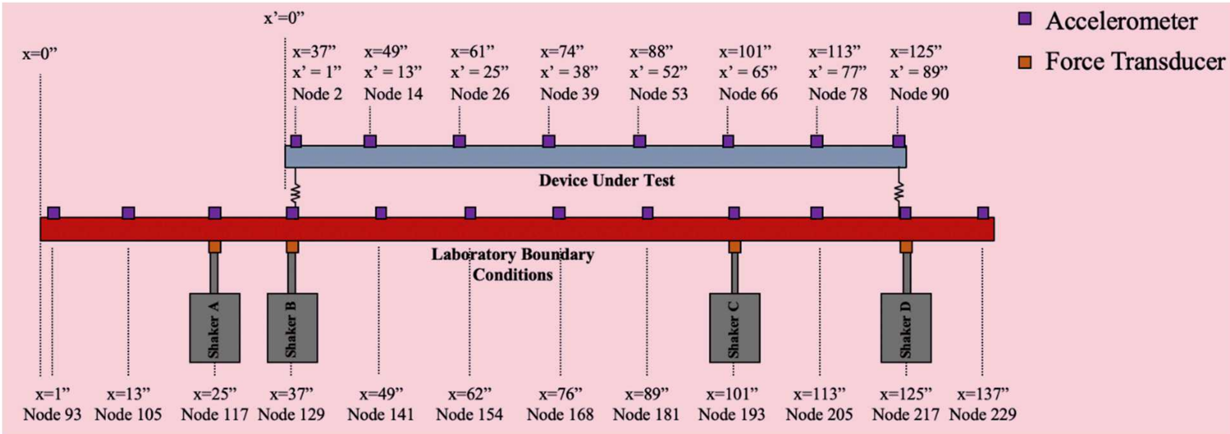

Figure 4: Laboratory Test Accelerometer and Shaker Placement

All eight nodes on the top beam were utilized as "*i*" DOFs. When exciting with shakers, the four DOFs on the bottom beam to which the shakers were attached were designated "*j*" DOFs. When exciting the field environment system with a hammer, node 229 on the right side of the lower beam was designated the "*j*" DOF where the hammer impact was applied.

SYSTEM CHARACTERIZATION

A 50 average burst random MIMO modal test was performed to extract mass normalized mode shapes and experimentally measured FRFs. The first 16 experimentally extracted mode shapes from the field environment configuration are shown in Table 1. Similarly, the first 18 experimentally extracted mode shapes from the laboratory test configuration are shown in Table 2.

Table 1: Field Environment Experimental Modal Model Mode Shapes

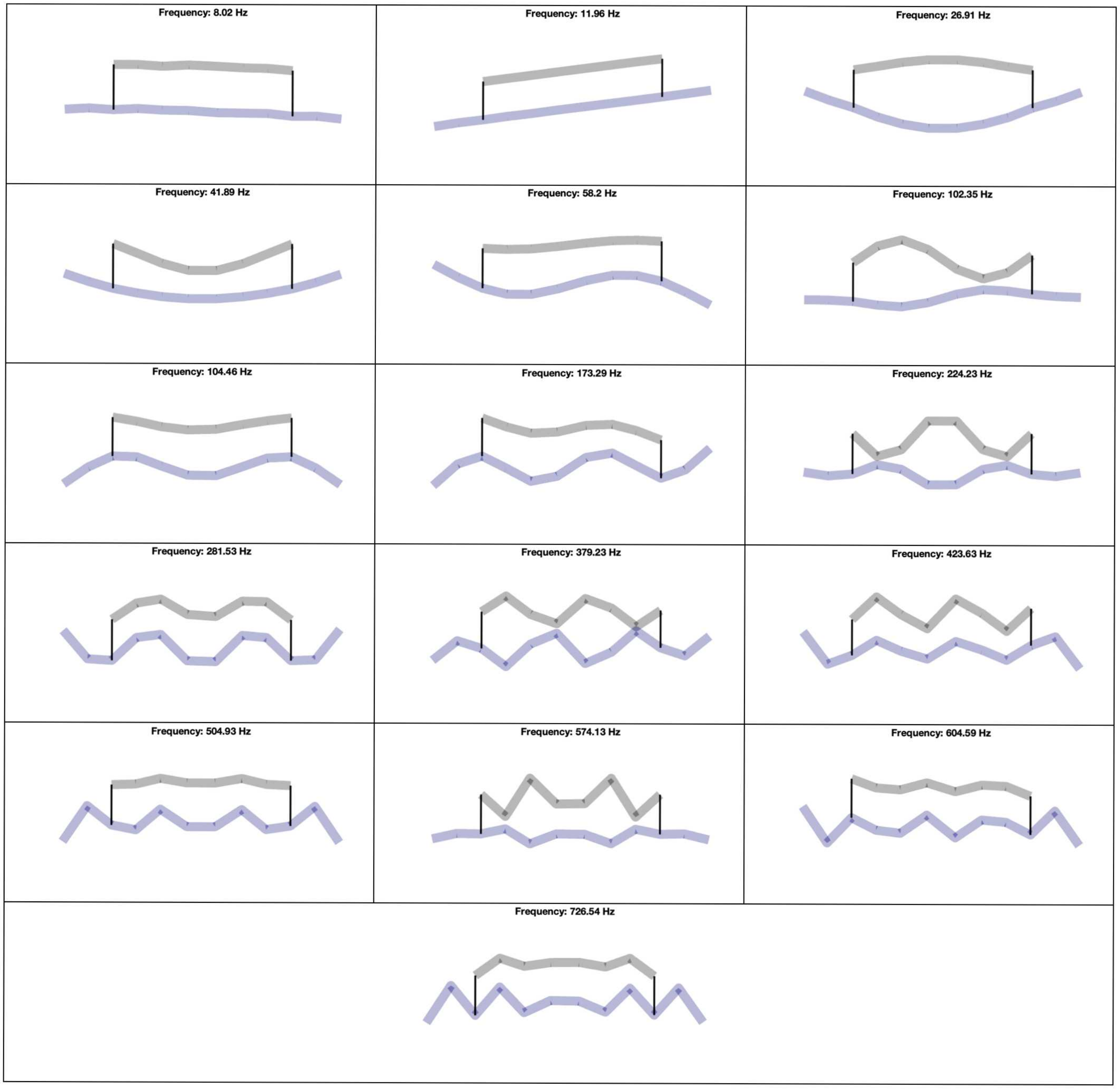

Table 2: Laboratory Test Experimental Modal Model Mode Shapes

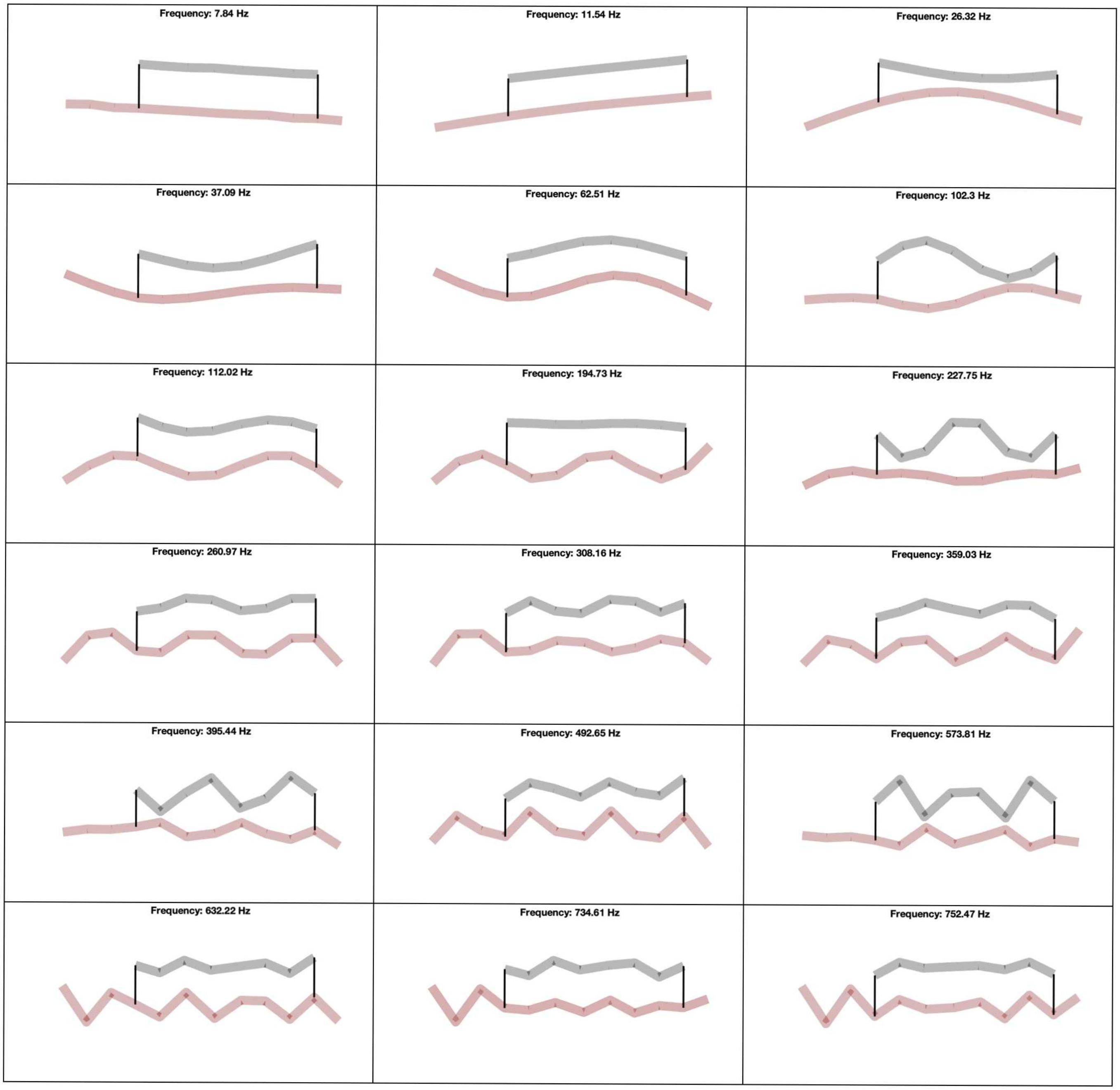

FRFs were synthesized from the resulting modal models and compared to the measured FRFs to ensure proper mode scaling and quality of modal parameter estimation. An example of one of the synthesized FRFs for the field environment configuration is shown in Figure 5 and for the laboratory test configuration in Figure 6.

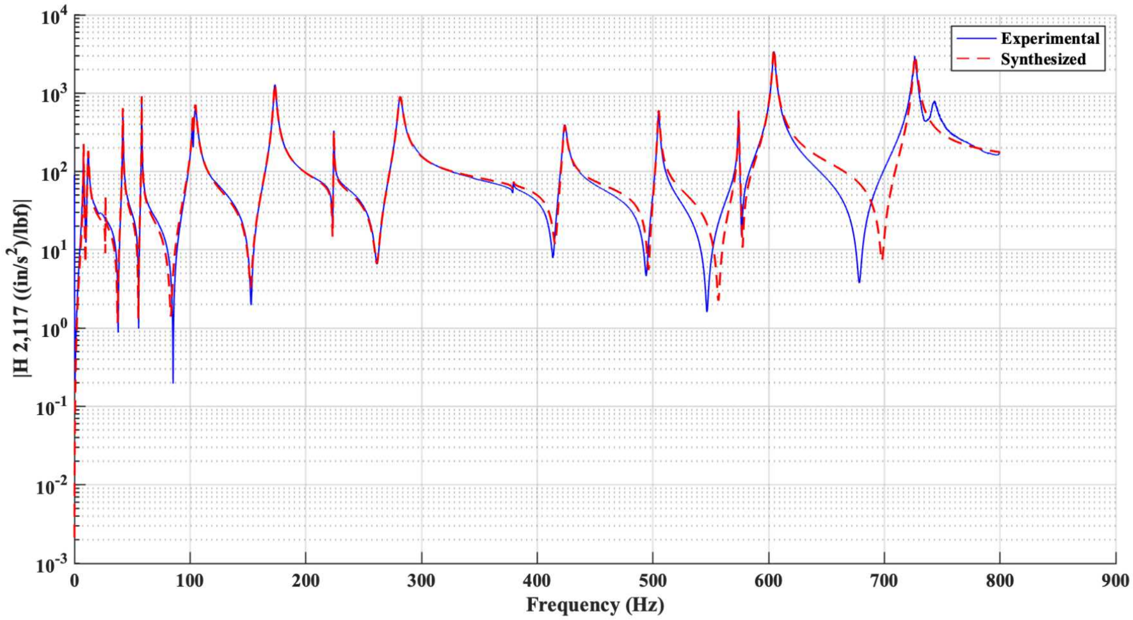

Figure 5: Experimental and Synthesized FRFs for Field Environment Configuration

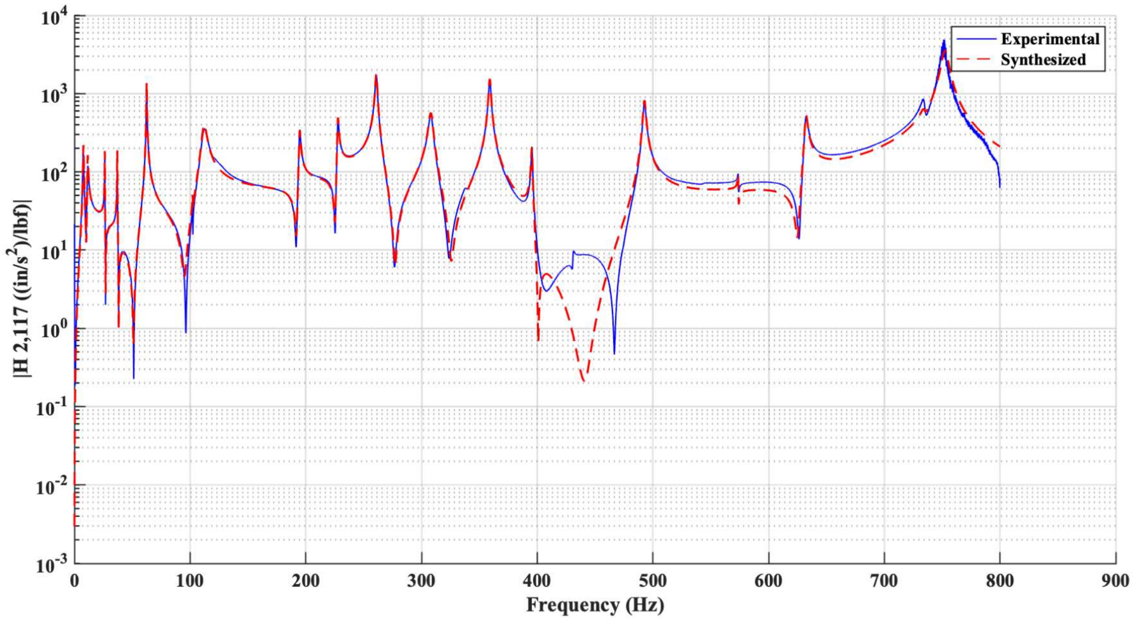

Figure 6: Experimental and Synthesized FRFs for Laboratory Test Configuration

In general, the synthesized FRFs matched the experimentally measured FRFs reasonably well with some discrepancies. There were some differences noted that were attributed to the absence of residual modes when developing the comparison.

FIELD ENVIRONMENT EXCITATIONS

Hammer Impulse Excitation

Two types of excitations were applied to the field environment system, an impulse force and a random/earthquake vibration signal. The impulse force was created by a soft-tip hammer hit at node 229 on the right side of the lower beam. The time history for the hammer impact force is shown in Figure 7 followed by the corresponding force spectra in Figure 8. The hammer excitation excited the system significantly out to about 500 Hz although the majority of the dynamics of the system responded below 300 Hz. The four shakers were not physically connected to the system during the hammer impact.

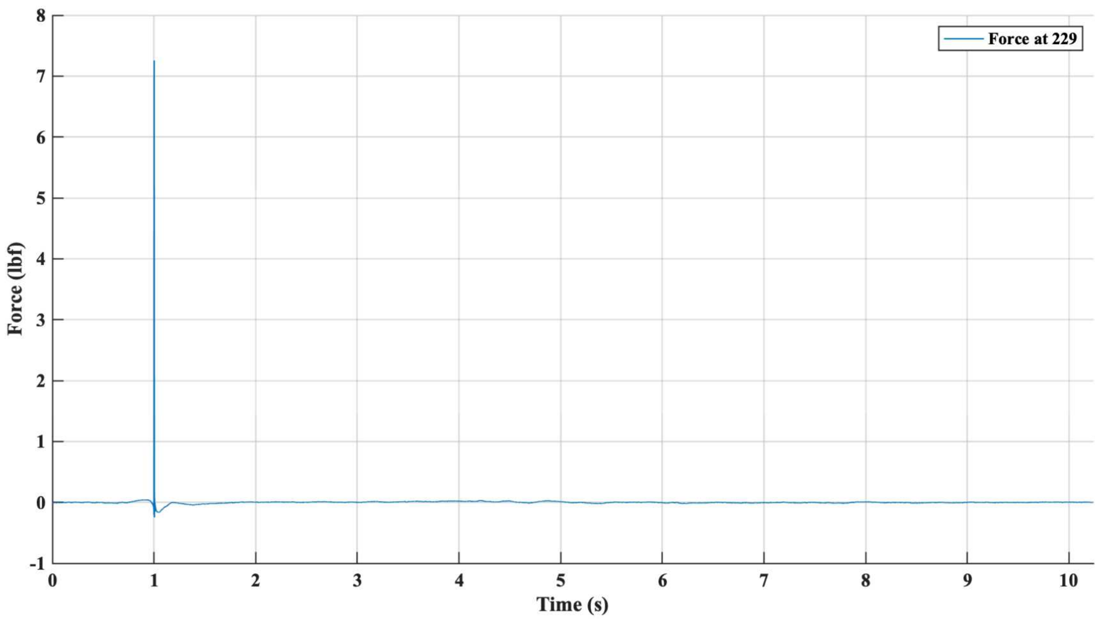

Figure 7: Field Environment Hammer Excitaiton Force

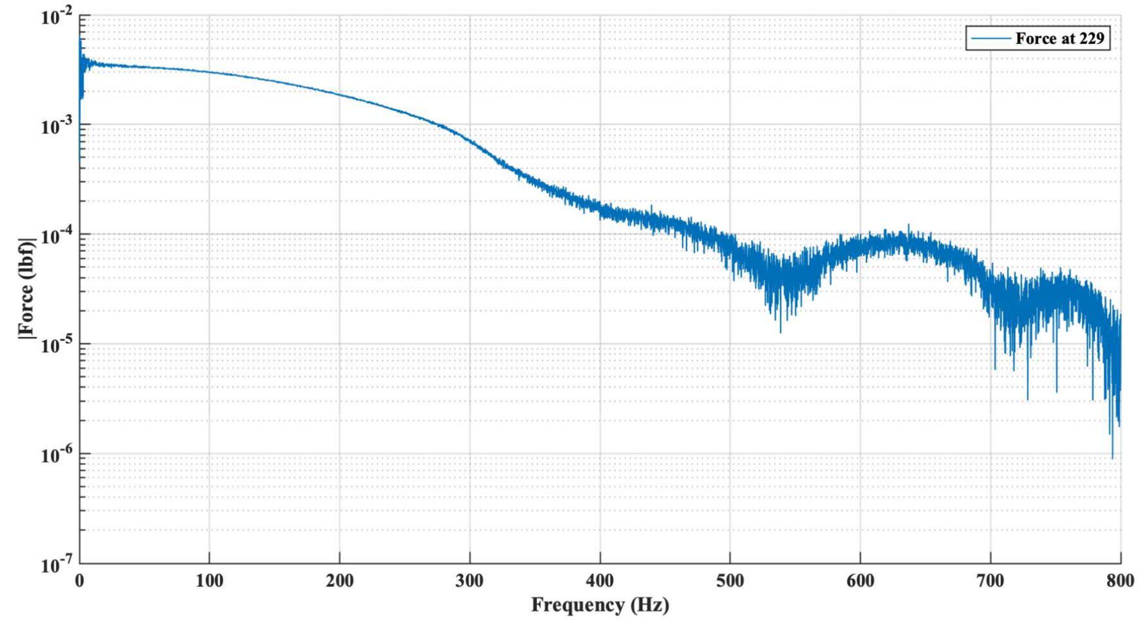

Figure 8: Field Environment Hammer Excitation Force Spectra

The response of the field environment system to the impact is shown at node 2 (on the left side of the DUT) in Figure 9 along with the corresponding response spectra in Figure 10.

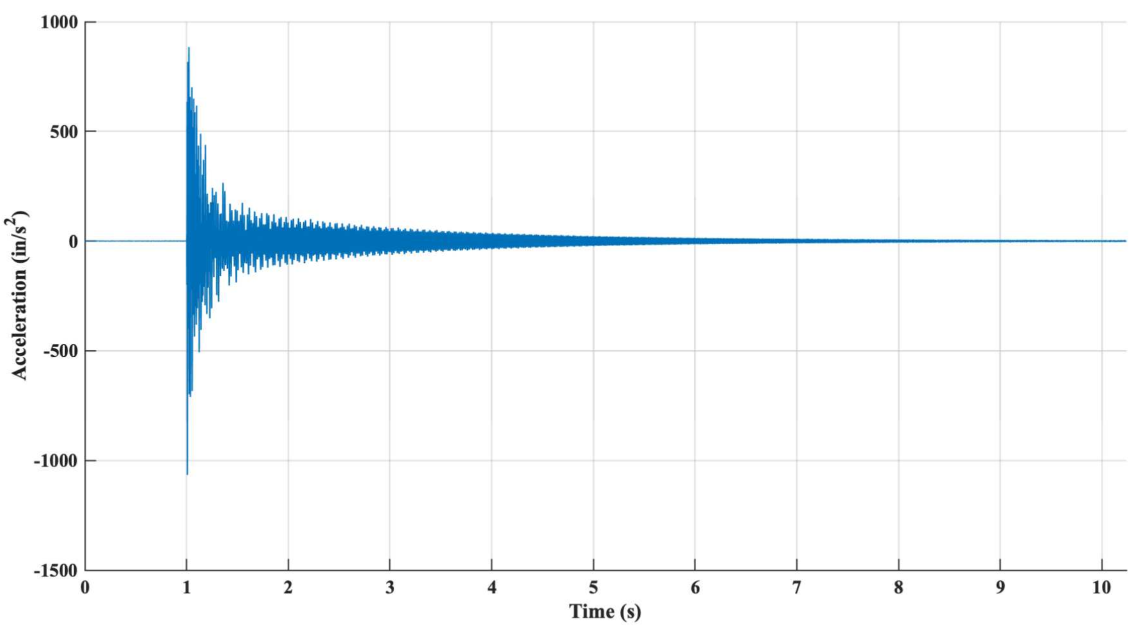

Figure 9: Field Environment Hammer Response at Node 2

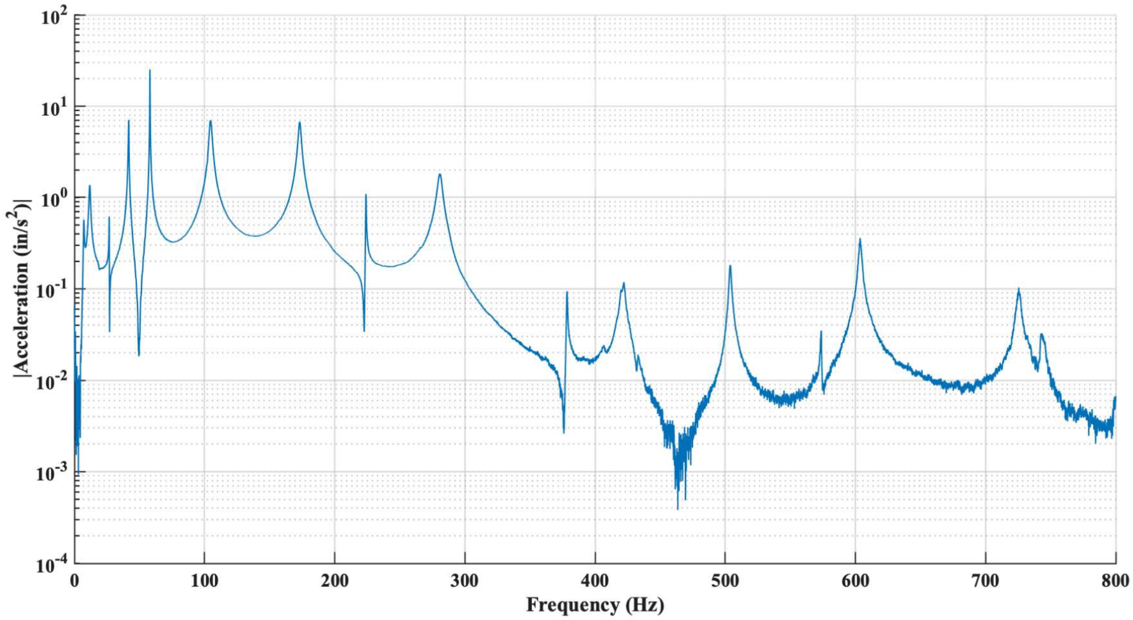

Figure 10: Field Environment Hammer Response Spectra at Node 2

Random/Earthquake Excitation

The random/earthquake excitation was created by providing an identical voltage signal to all four shakers at the same time (coherent signals). The signal was generated using a modified version of the El-Centro earthquake response profile as a voltage signal. The time history for the resulting shaker voltage is shown in Figure 11 followed by the corresponding voltage spectra in Figure 12. The random/earthquake excitation signal provided a broad excitation of the structure throughout the measured 800 Hz bandwidth of the test.

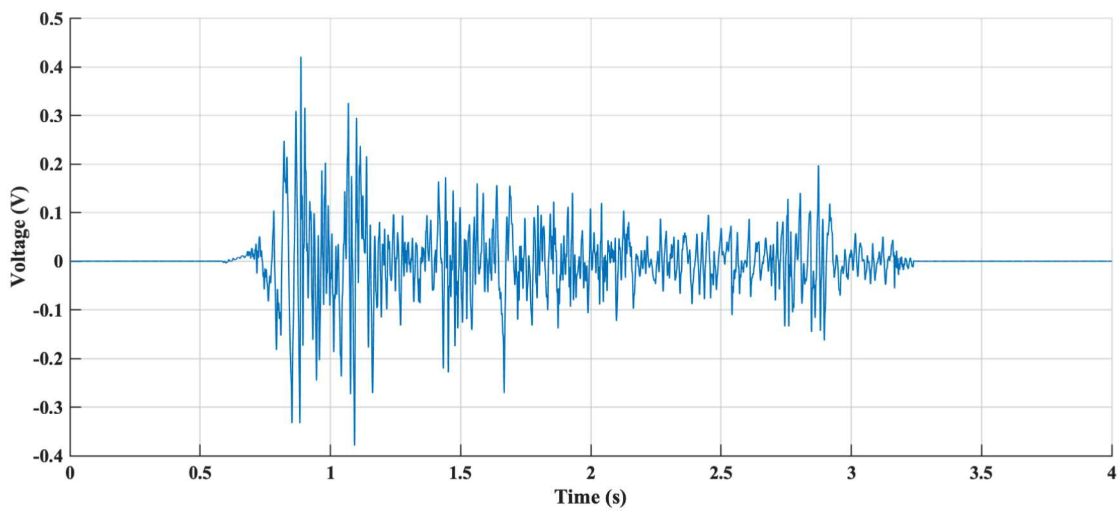

Figure 11: Field Environment Random/Earthquake Excitation Voltage

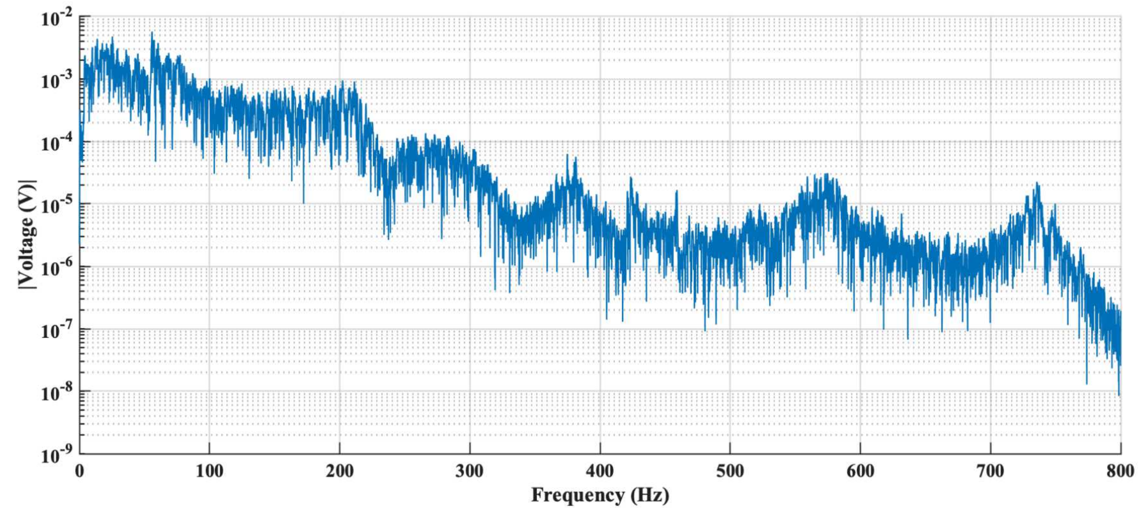

Figure 12: Field Environment Random/Earthquake Excitation Voltage Spectra

The response of the field environment system to the random/earthquake excitation is shown at node 2 (on the left side of the DUT) in Figure 13 along with the corresponding response spectra in Figure 14. Once again, a large portion of the response occurred below 300 Hz.

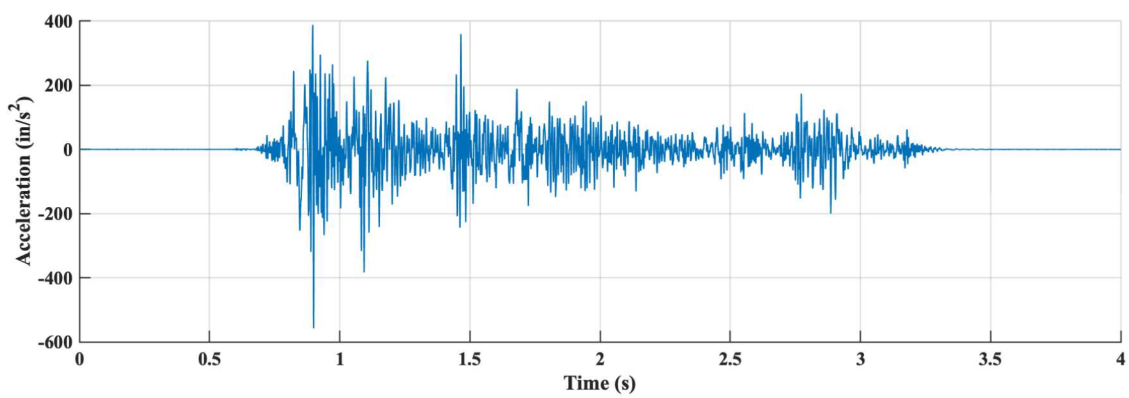

Figure 13: Field Environment Random/Earthquake Response at Node 2

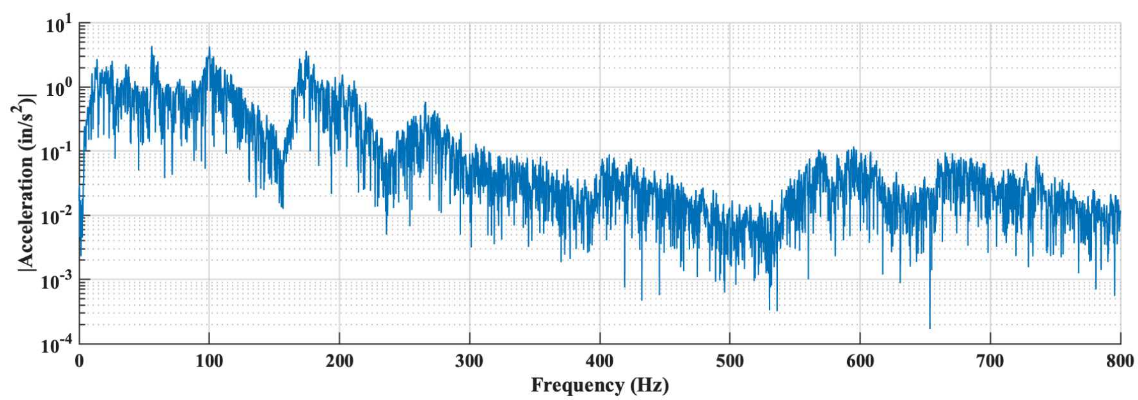

Figure 14: Field Environment Random/Earthquake Response Spectra at Node 2

MODAL AMPLITUDE CONTRIBUTATION MATRIX (MACM)

Hammer Impulse MACM

The MACM for the hammer impulse excitation was calculated using modal parameters extracted from the experimentally collected FRFs. The MACM describes which field environment modes and laboratory test modes are important to replicating the dynamics of the field system in the laboratory. All eight reference accelerometers were utilized when calculating the MACM, however as few as four could have been used and similar results would have been expected.

The an isometric view of the MACM for the hammer impulse excitation is shown in Figure 15, the field environment mode view in Figure 16, and the laboratory test mode view in Figure 17.

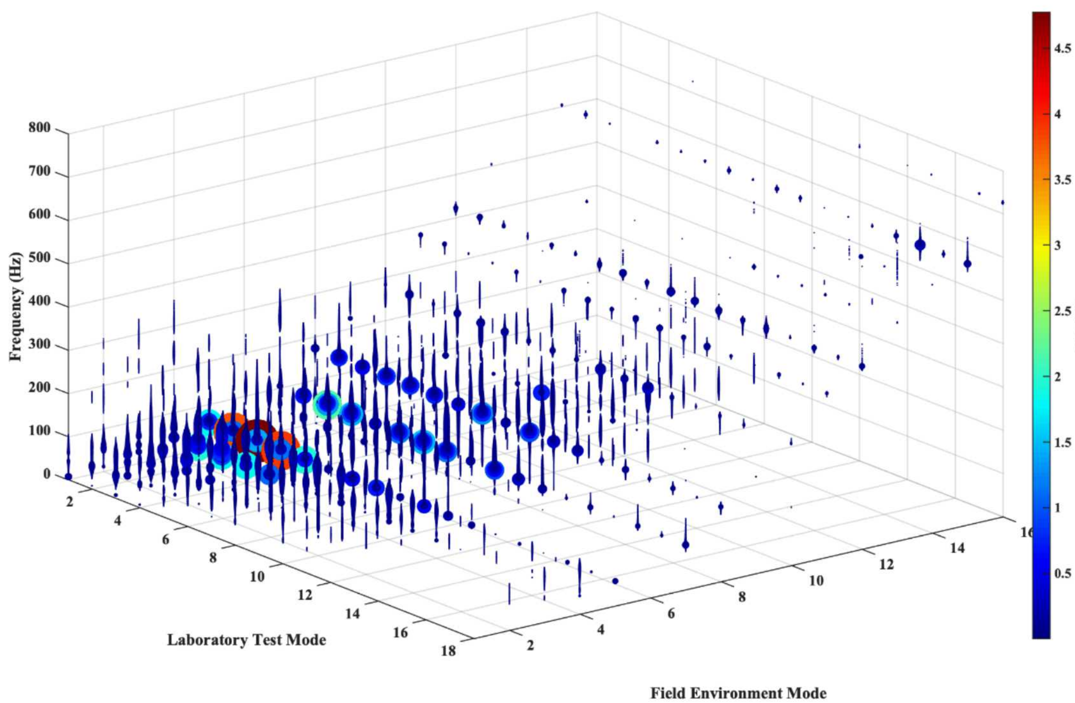

Figure 15: MACM for Hammer Impact (Isometric View)

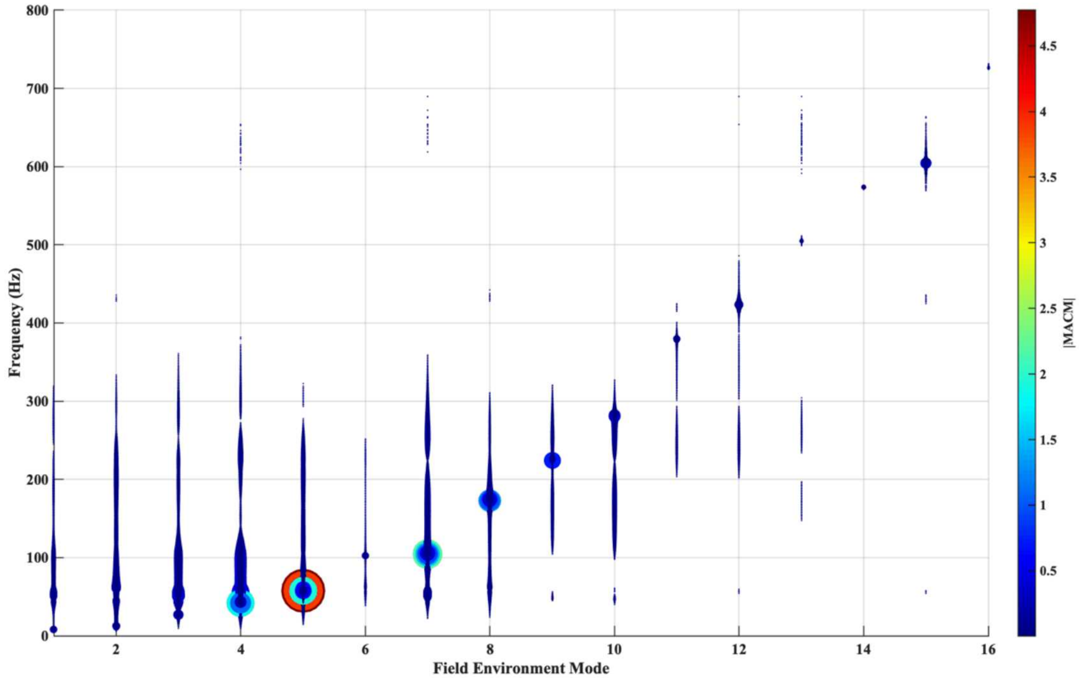

Figure 16: MACM for Hammer Impact (Field Environment Mode View)

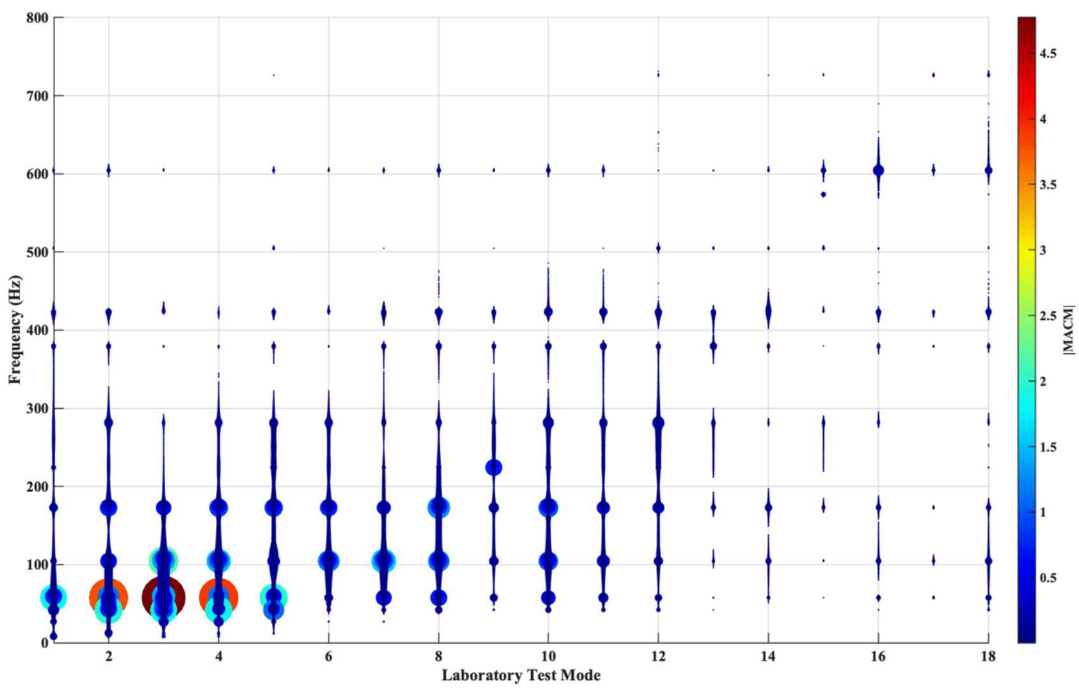

Figure 17: MACM for Hammer Impact (Laboratory Test Mode View)

The MACM plots for the hammer impact were studied to determine a truncated set of modes that could excite the majority of the dynamics of the system. A goal was set to try to match the dynamics at 300 Hz and below as best as possible using a specified set of truncated modes. From the field environment view in Figure 16, the large circles in the lower left quadrant of the plot demonstrate the important modes for matching the dynamics below 300 Hz. The first 10 field environment modes had noticeably larger MACM values than the higher order modes in the 0 to 300 Hz range. From the laboratory test view in Figure 17, the large circles in the lower left quadrant of the plot demonstrate the importance of the first 12 laboratory test modes. Therefore, the first 12 laboratory test modes were selected for the truncated set to capture the majority of the dynamics below 300 Hz. For one of the excitation cases, voltages were calculated using the truncated set of the resulting 10 field environment modes and 12 laboratory test modes identified from the MACM.

Random/Earthquake MACM

Just as the MACM for the hammer impulse, the MACM for the random/earthquake excitation was calculated using modal parameters extracted from the experimentally collected FRFs. Once again, all eight reference accelerometers were utilized when calculating the MACM.

The an isometric view of the MACM for the random/earthquake excitation is shown in Figure 18, the field environment mode view in Figure 19, and the laboratory test mode view in Figure 20.

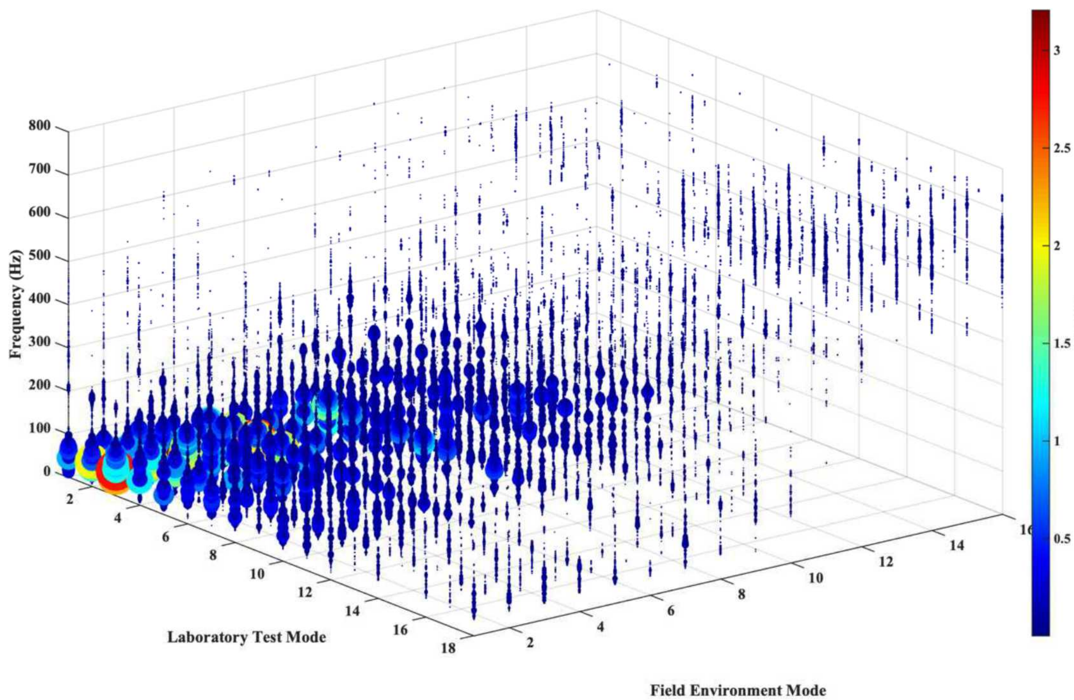

Figure 18: MACM for Random/Earthquake (Isometric View)

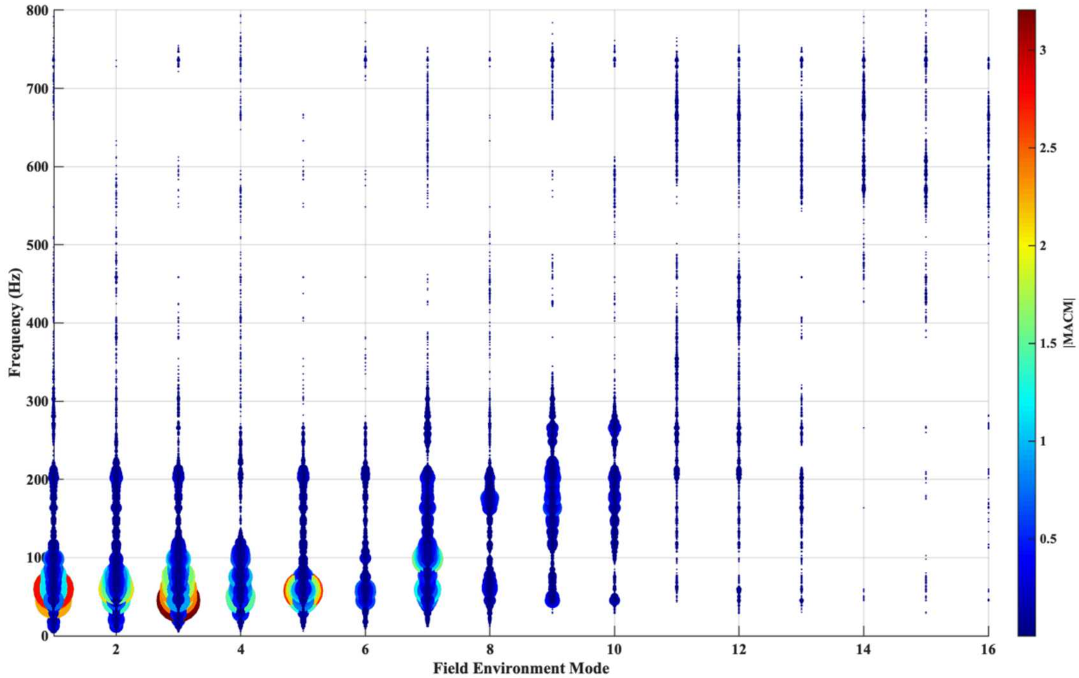

Figure 19: MACM for Random/Earthquake (Field Environment Mode View)

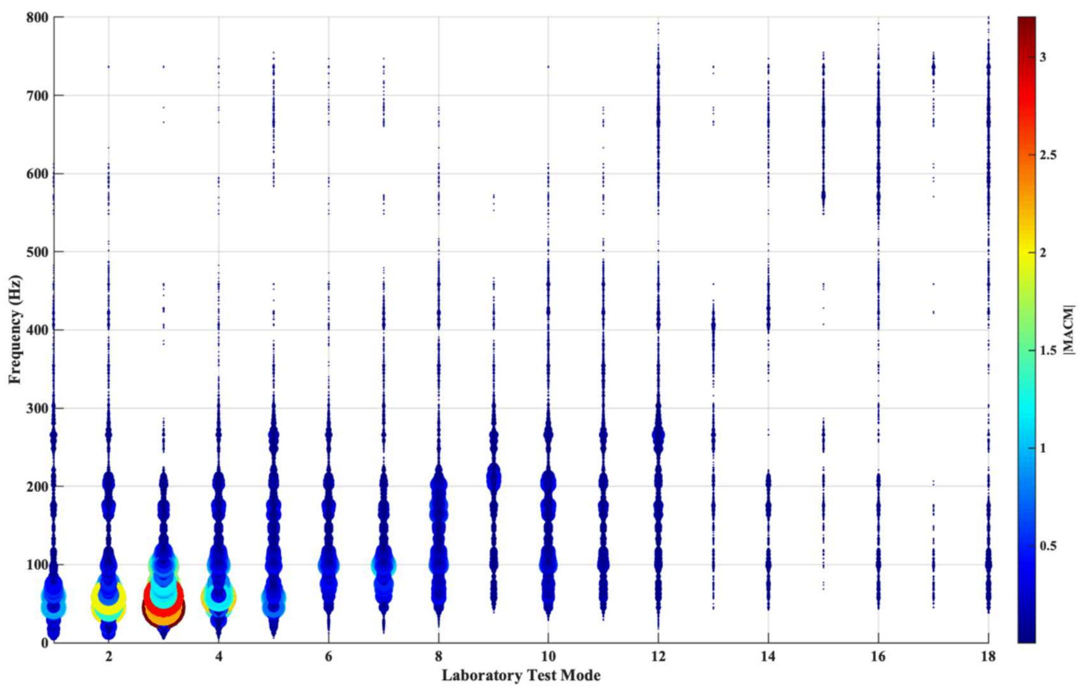

Figure 20: MACM for Random/Earthquake (Laboratory Test Mode View)

The MACM plots for the random/earthquake excitation were studied to determine a truncated set of modes that could excite the majority of the required dynamics to accurately replicate the field response. Once again, a goal was to try to match the dynamics at 300 Hz and below as best as possible using a specified set of truncated modes. From the field environment view in Figure 19, the large circles in the lower left quadrant of the plot demonstrate the importance of first 10 field environment modes to the dynamics from 0 to 300 Hz. From the laboratory test view in Figure 20, the large circles in the lower left quadrant of the plot demonstrate the importance of the first 12 laboratory test modes in the 0 to 300 Hz range. For one of the excitation cases, voltages were calculated using the truncated set of the resulting 10 field environment modes and 12 laboratory test modes identified from the MACM just as they were for the impact environment.

RESULTS

Hammer Impulse Results

Shaker voltages were computed utilizing Equation 5, however the FRFs utilized in Equation 5 came from three sources. The first method directly utilized the experimentally measured FRFs between force and acceleration. The second method used synthesized FRF from an experimental modal model. The third method utilized synthesized FRFs from a truncated set of modes selected based on the MACM plots from Figure 15 through Figure 20. The voltages were applied to the shakers and the acceleration responses at all 20 accelerometers was recorded. The resulting eight laboratory test DUT response measurements were then compared to the reference field environment response measurements to see how well the field response was replicated in the laboratory.

The resulting DUT response spectra for both the field and laboratory are shown in Figure 21 when utilizing experimental FRFs, Figure 22 when utilizing synthesized FRFs, and Figure 23 when utilizing synthesized FRFs with the truncated set of modes. The truncated set of modes included the first 10 field environment modes and the first 12 laboratory test modes as indicated by Figure 16 and Figure 17. The MACM indicated that the selection of truncated modes would largely capture the dynamics necessary to re-create the response of the field environment DUT in the laboratory test.

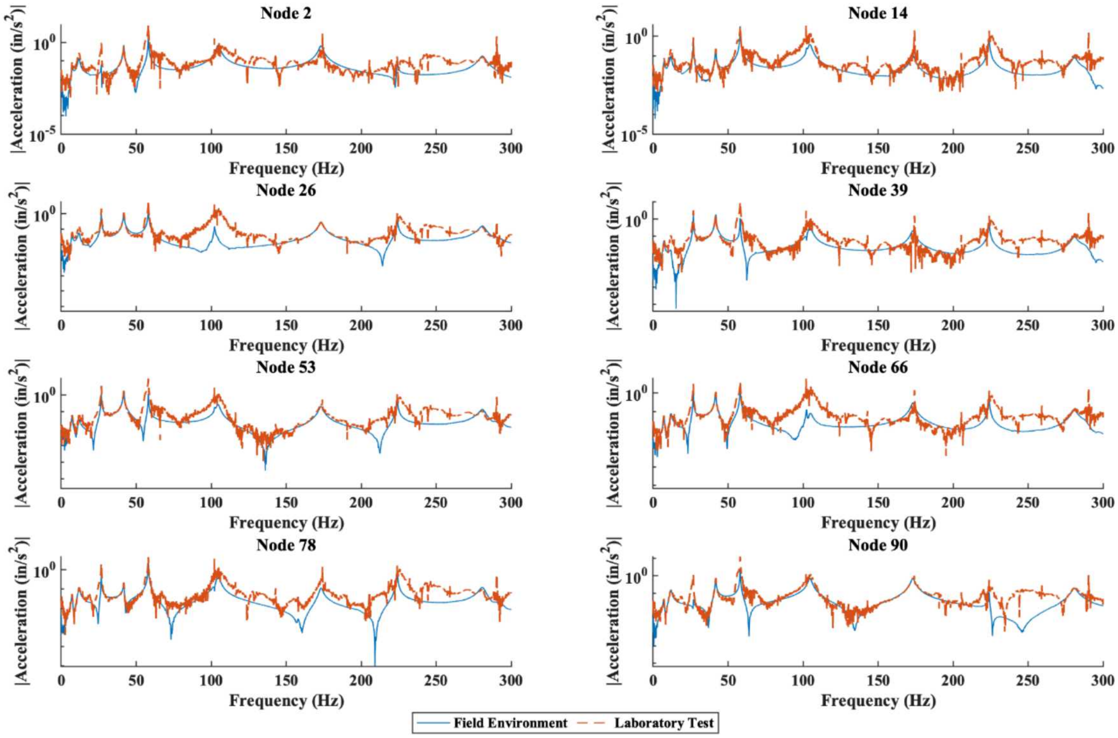

Figure 21: Hammer Impact Field and Laboratory DUT Response Spectra
(Voltages Computed using Experimentally Measured FRFs)

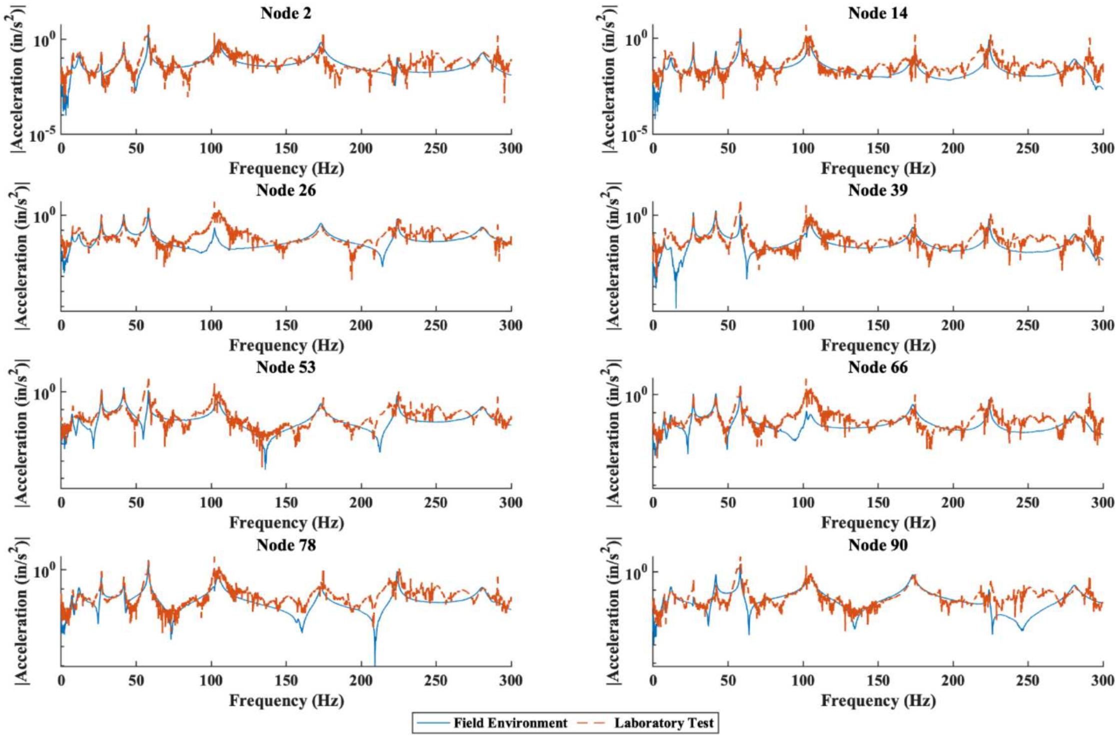

Figure 22: Hammer Impact Field and Laboratory DUT Response Spectra
(Voltages Computed using FRFs Synthesized from Experimental Modal Model)

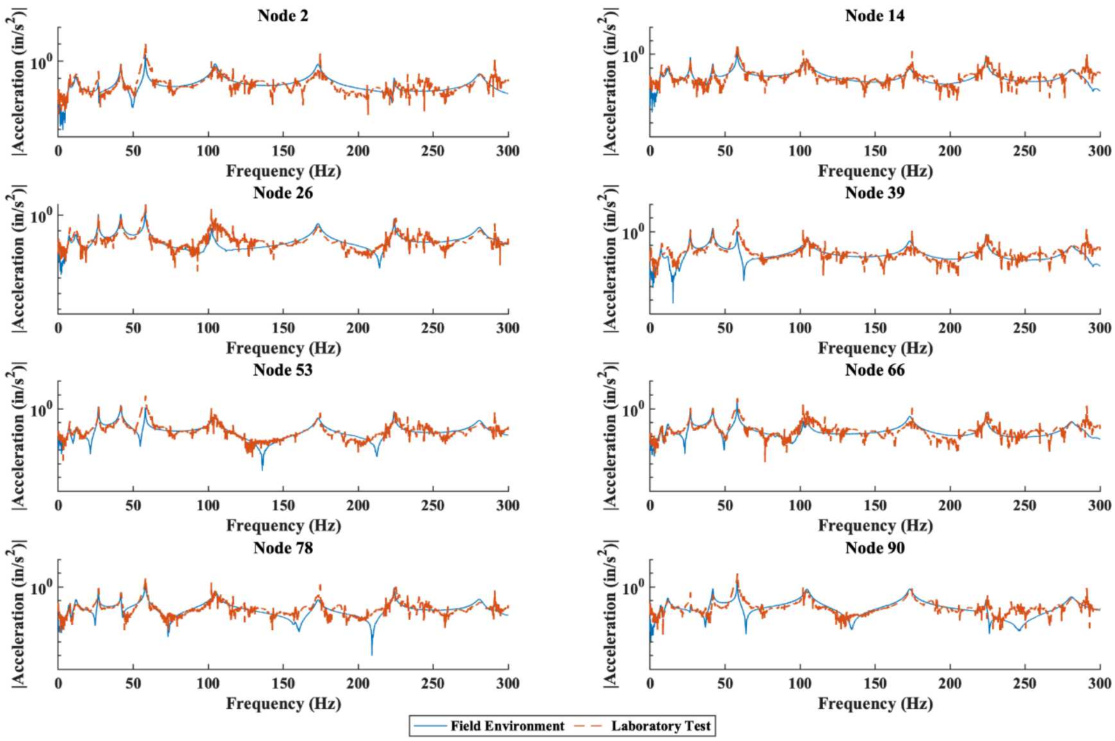

Figure 23: Hammer Impact Field and Laboratory DUT Response Spectra
(Voltages Computed using FRFs Synthesized from Truncated Experimental Modal Model)

Results shown in Figure 21, Figure 22, and Figure 23 show a reasonable replication of the field environment DUT response in the laboratory on a DUT with severely modified flexible boundary condition. The spectra appear slightly noisy because no averaging was utilized for the reference field environment DUT response nor was averaging utilized when measuring the laboratory test DUT response. All three methods of computing voltages resulted in roughly similar response replication quality, although the truncated set of responses appears marginally improved compared to the other two.

The fact that the truncated set of modes replicated the field environment as well as the non-truncated set demonstrates that the MACM was useful tool to correctly identify which modes are imperative to measure, excite, or model in the field and laboratory system.

Random/Earthquake Results

The computations for replicating the random/earthquake response were identical to those for the replication of the hammer impulse. The resulting responses for both the field and laboratory DUT response spectra are shown in Figure 24 when computing excitation voltages utilizing synthesized FRFs with a truncated set of modes.

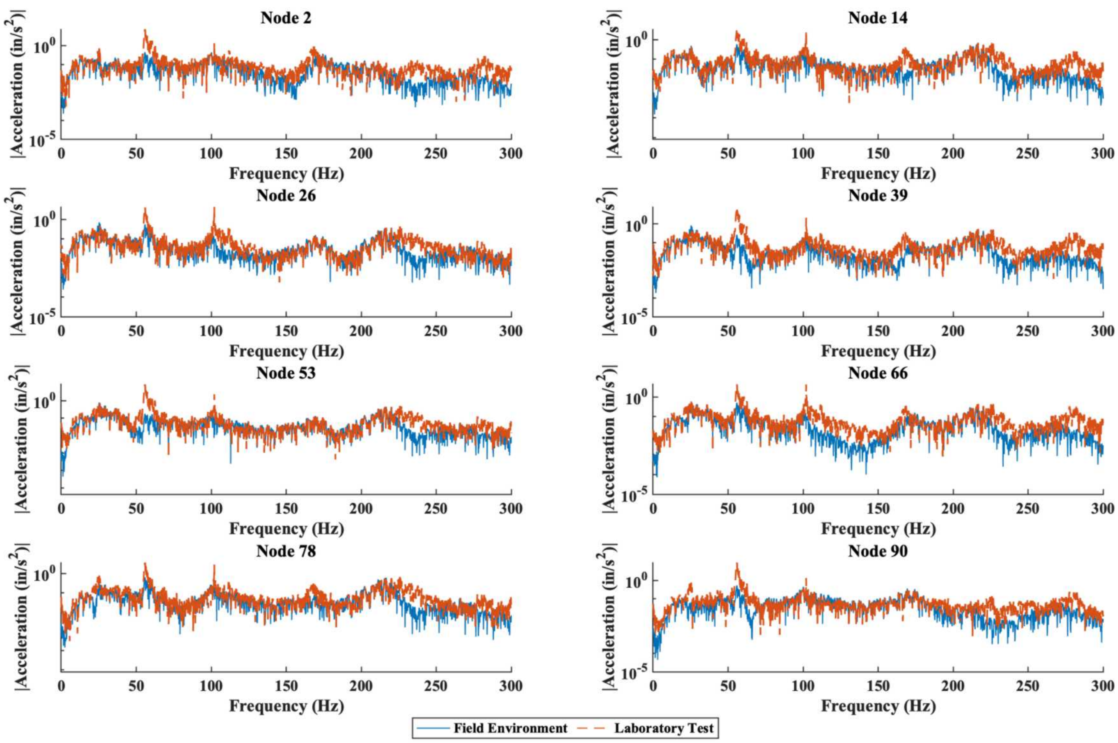

Figure 24: Random/Earthquake Field and Laboratory DUT Response Spectra
(Voltages Computed using FRFs Synthesized from Truncated Experimental Modal Model)

Both the hammer impulse and the random/earthquake replications had noticeable errors in the 60 Hz bandwidth region. There is a lightly damped mode of the laboratory test system at 62.5 Hz with 0.3% damping that has been over-excited during the laboratory test replication of the field environment dynamics. The cause of the over-excitation at some frequency bands is thought to be due to phase errors between the expected response and the actual response of the system and will be investigated further in future work.

In general, both the hammer impulse field environment and the random/earthquake field environment DUT responses were replicated reasonably well in the laboratory test. The boundary condition changes introduced in the laboratory test configuration for the DUT were compensated for and the resulting DUT responses in the laboratory test reasonably replicated the DUT response from the field environment for much of the frequency range of the test.

The ability to selectively truncate the models of the field and laboratory system, by identifying the most important modes to the replication of the field environment dynamics in the laboratory configuration, was demonstrated experimentally. The truncation of the modal model based on the MACM did not appear to negatively impact the ability to replicate the field environment response of the DUT in the laboratory configuration.

CONCLUSION

This paper demonstrated an experimental method to replicate a field environment response in a laboratory setting compensating for boundary condition differences between field and laboratory. The method was applied for a shock impulse type of excitation as well as for a random/earthquake vibration signature. A fairly severe boundary condition difference was created in the experimental setup by mounting the DUT in a geometrically different location.

Two variations of FRF synthesis were tested, including utilizing experimental FRFs and utilizing FRFs synthesized from an experimental based modal model. The methods tested were found to have a rather small effect on the overall results.

A physics-based map between field environment modes and laboratory test modes, called the MACM, was calculated from experimental data and utilized to truncate the number of modes accounted for in the laboratory test excitation to a minimum set. The truncated set of results was found to perform as good or better than the methods accounting for the full bandwidth of dynamics which increases confidence that MACM map utilized is accurate for experimental application.

DUT dynamics were replicated in the laboratory environment with reasonable accuracy. The replication of the dynamics was inaccurate for some frequency ranges that appeared to correlate with lightly damped modes of the laboratory test system. Further studies are anticipated to study this technique in more depth and with a variety of different DUT/fixture scenarios. Overall, the DUT dynamics were replicated well considering the severe boundary condition difference implemented between the field and laboratory configurations studied in this work.

ACKNOWLEDGEMENTS

This work was inspired by the methods presented by Phil Daborn at the Atomic Weapons Establishment, Jesus Reyes-Blanco at University of Massachusetts at Lowell, and Randy Mayes and Tyler Schoenherr at Sandia National Laboratories. Funding for this work was graciously provided by Sandia National Laboratories.

REFERENCES

[1] T. D. Scharton, Force Limited Vibration Testing Monograph, Pasadena, CA: Jet Propulsion Laboratory, California Institute of Technology, 1997.

[2] P. M. Daborn, Smarter Dynamic Testing of Critical Structures, Bristol, England: University of Bristol, 2014.

[3] P. Avitabile, "Why you can't ignore those vibration fixture resonances," *Sound and Vibration,* vol. 33, pp. 20-27, 1999.

[4] P. M. Daborn, P. R. Ind and D. J. Ewins, "Enhanced ground-based vibration testing for aerodynamic environments," *Mechanical Systems and Signal Processing,* vol. 49, pp. 165-180, 2014.

[5] P. M. Daborn, C. Roberts, D. J. Ewins and P. R. Ind, "Next-Generation Random Vibration Tests," in *Proceedings of the 32nd International Modal Analysis Conference*, Orlando, FL, 2014.

[6] J. M. Reyes-Blanco, "Adjustment of Vibration Response to Account for Fixture-Test Article Dynamic Coupling Effects," in *Proceedings of the 35th International Modal Analysis Conference*, Garden Grove, CA, 2017.

[7] R. L. Mayes, "A Craig-Bampton Experimental Dynamic Substructure using the Transmission Simulator Method," in *Proceedings of the 33rd International Modal Analysis Conference*, Orlando, FL, 2015.

[8] R. L. Mayes, "A Modal Craig-Bampton Substructure for Experiments, Analysis, Control and Specifications," in *Proceedings of the 33rd International Modal Analysis Conference*, Orlando, FL, 2015.

[9] B. R. Zwink, P. Avitabile and D. G. Tipton, "Modal Projection Matching," in *Proceedings of the 37th International Modal Analysis Conference*, Orlando, FL, 2019.

[10] B. R. Zwink, B. Daniels, P. Avitabile and D. G. Tipton, "Boundary Condition Compensation Map," in *Proceedings of the 38th International Modal Analysis Conference*, Houston, TX, 2020.

[11] P. Avitabile, *MECH 5150 Course Notes,* Lowell, MA: University of Massachusetts Lowell, 2017.

[12] T. F. Schoenherr, "Quantification of Modal Truncation Error with Respect to a Test Fixture's Ability to Replicate a Structural Dynamic Environment," in *Proceedings of the 37th International Modal Analysis Conference*, Orlando, FL, 2019.

[13] P. Avitabile, Modal Testing: A Practitioner's Guide, Lowell, MA: The Society for Experimental Mechanics and John Wiley & Sons Ltd., 2018.

This manuscript has been authored by National Technology and Engineering Solutions of Sandia, LLC. under Contract No. DE-NA0003525 with the U.S. Department of Energy/National Nuclear Security Administration. The United States Government retains and the publisher, by accepting the article for publication, acknowledges that the United States Government retains a non-exclusive, paid-up, irrevocable, world-wide license to publish or reproduce the published form of this manuscript, or allow others to do so, for United States Government purposes.